Table S1. Combinations of fluorochrome-conjugated antibodies used in panels for this study

Fluorochrome	*T-cell differentiation*	*T-cell activation*	*DC / B / Mono*	*NK-cells*	*Tregs*	*T function*	*NK function*
Cy55PerCP			CD3	CD3			
FITC	CD45RA	Ki-67	CD16	CD16	Ki-67		IFN-γ
CY7 APC	CD3	CD3	CD20	CD20	CD3	CD3	CD3
Alexa 680	CD27	CD38	CD27	CD8b		CCR7	MIP-1β
APC	CD95	CCR5	CD11c			CD95	
Qdot 800	CD8	CD8	CD8	CD8	CD8	CD8	
Qdot 655	CD4	CD122	CD14	CD122		CD45RA	CD8
Qdot 605	CD28	CD4	CD4	CD4	CD4		
Qdot 545		HLA-DR	HLA-DR			CD4	
ViViD Pacific Blue	ViViD +CD14	ViViD +CD14	ViViD +CD16	ViViD +CD14	ViViD +CD14	ViViD +CD14	ViViD +CD14
CY7 PE		CD25	CD86		CD25	TNF-α	TNF-α
Alexa 700-PE							CD20
CY5 PE		CD95	CD80	CD56	FoxP3	CD28	CD16
Alexa 594	CCR7	CCR7				IFN-γ	CD56
PE	CD127	CD132	IL-15Ra	CD132	CD127	IL-2	NKG2D

Figure S1. Representative example of CD132 and CD122 expression in different subsets of NK- and T cells at the steady state. NK-cells were defined as depicted in Fig. 2A; T_N, T_{CM} and T_{EM} cells on the basis of CCR7 and CD95 expression, as in Fig. 3A.

Figure S2. Effect of IL-15 on the quality of T- and NK- cell functional responses (A) Frequency of responding CD4+ and CD8+ T cells after overnight polyclonal stimulation, as revealed by the production of IL-2, IFN-g and TNF-a production. (B) Bar charts of the quality of the CD4+ and CD8+ T-cell response after Boolean gating of cells producing IL-2, IFN-g or TNF-a. (C) Frequency of responding NK-cell subsets after overnight polyclonal stimulation, as revealed by the analysis of MIP-1b, IFN-g and TNF-a production. (D–E) Bar and pie charts of the quality of the cytokine-response in CD56-CD16- (D) and CD56-CD16+ (E) NK cells after Boolean gating of cells producing MIP-1b, IFN-g or TNF-a. ⁎, $P<0.05$ after Wilcoxon rank test vs. d-7. 2: IL-2; g: IFN-g; T: TNF-a, M: MIP-1b.

Figure S3. IL-15 expands natural occurring regulatory T (Tregs) cells but does not lead to their long-lasting accumulation. (A) Gating strategy for the identification of Tregs: CD4+ T cells were identified as in Fig. 2C, Tregs were further defined as CD25+, FoxP3+ and CD127-. The fraction of proliferating, Ki-67+ Tregs was subsequently determined. CD127 and Ki-67 expression in Tregs (red dots) are overlayed to conventional CD4+ cells (black contour) for comparison. (B) Dynamics of Treg and Ki-67+ Treg expansion in IL-15-treated animals. (C) Frequency of Tregs and Ki-67+ Tregs in multiple tissues at d13 and d48 after the first IL-15 injection. Data were expressed as in Fig. 3B. Tissue abbreviations were reported as indicated in Materials and methods. ⁎, $P<0.05$ after Wilcoxon rank test vs. d-7 (B) or vs. sham (C).

Figure S4. IL-15 administration alters the homeostasis of DC subsets. a) Gating strategy used for the identification of DC subsets. DCs were defined as those cells not expressing CD16, CD14, CD3, CD20 but positive for HLA-DR. Plasmacytoid DC (pDCs) selectively express CD123 while myeloid DC (mDCs) CD11c. Levels of CD80, CD86 and IL-15Ra were shown in both subsets (indicated in red for pDCs and in blue for mDCs). Monocytes were defined as CD14+ and levels of IL-15Ra expression in these cells is also shown. (B) The relative change in the absolute counts of circulating pDCs and mDCs upon IL-15 treatment is shown. Counts were obtained and indicated as described in Fig. 1. *, $P<0.05$ for Wilcoxon rank test in IL-15-treated vs. sham. (C) Representative example of the frequency of NKT cells (defined as PBS57/CD1d-tetramer+ Va24+) in the peripheral blood of a RM treated with 10 mg/Kg IL-15. Live CD3+ CD14- CD20- are shown.

Figure S5. Little activation of T_N cells in response to IL-15 treatment. Ki-67 (percentage of cells) and CD122 (MFI values) expression in T_N as found in multiple tissues at d13 after IL-15 administration. T_N were defined as those expressing CCR7 but not CD95. Data were expressed as indicated in Fig. 3B.

Figure S6. Proliferation and activation of T cell is normalized at d48 after initiation of IL-15 treatment. Frequency of T_{CM} (CCR7+CD95+) and T_{EM} (CCR7-CD95+) T-cells expressing Ki-67 and CD25 (CD4+) or Ki-67 and CD38 (CD8+) in different tissues of the body at d48 after IL-15 treatment initiation. Expression of CD122 (MFI) was also shown in the same cell subsets. Data were expressed as in Fig. 3B. Tissue abbreviations were reported as indicated in Materials and methods.

Figure S7. Spontaneous annexin V (anxV) expression on naïve, T_{CM} and T_{EM} cells after 24 hours culture. T-cell differentiation state was determined as in Fig. S5.

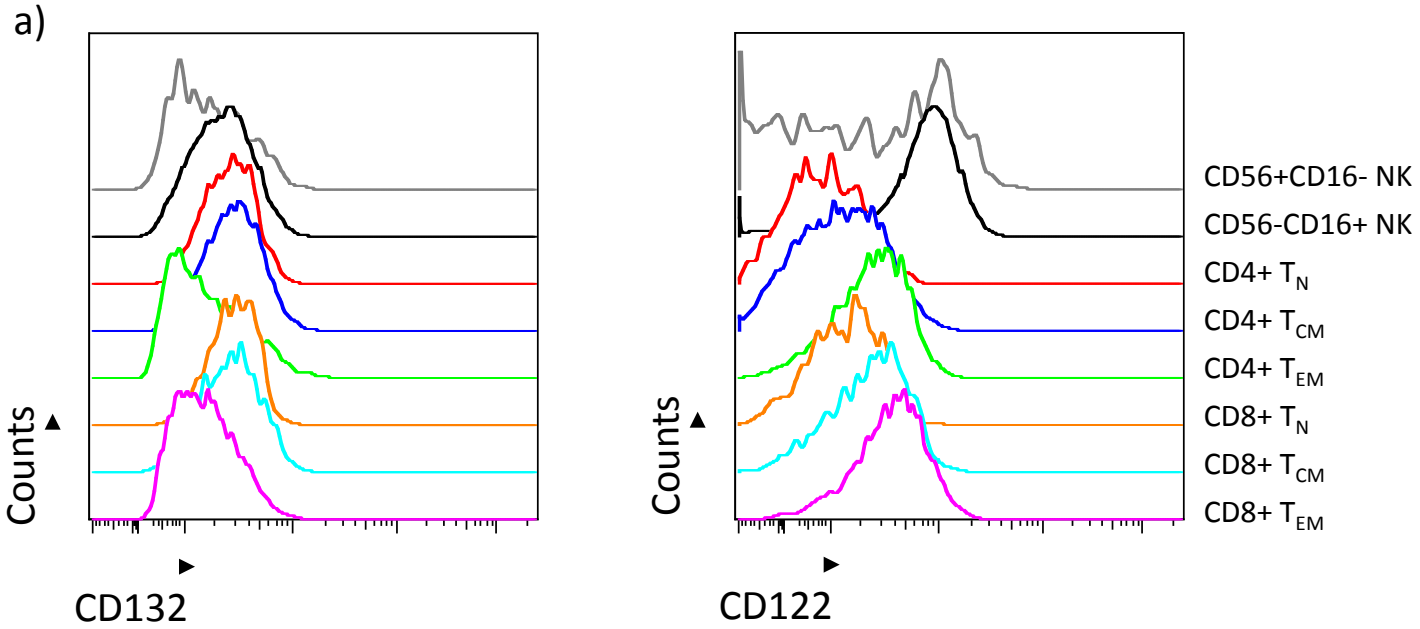
a)
Counts
CD132
Counts
CD122
CD56+CD16- NK
CD56-CD16+ NK
CD4+ T_N
CD4+ T_{CM}
CD4+ T_{EM}
CD8+ T_N
CD8+ T_{CM}
CD8+ T_{EM}

Figure S1

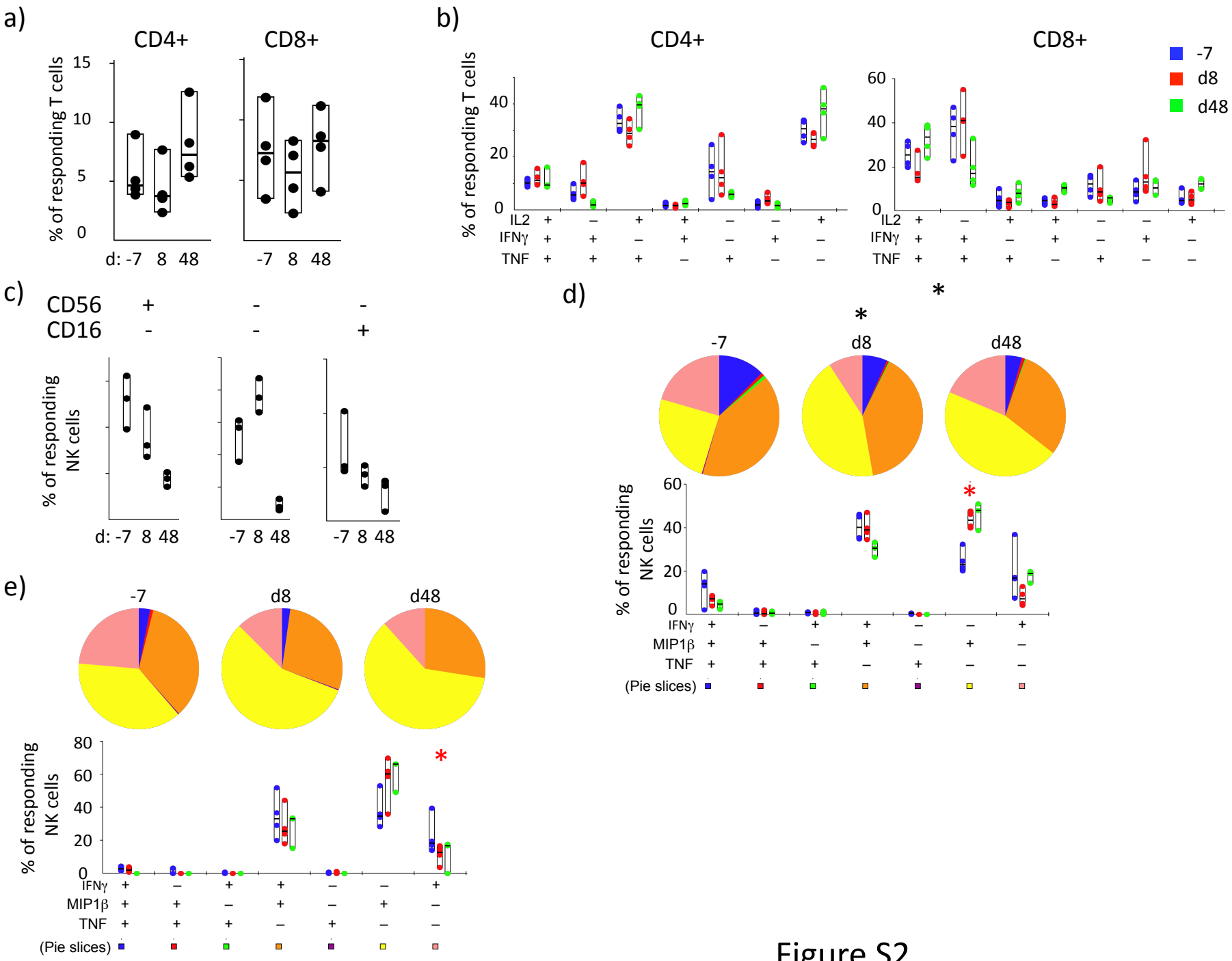
a)
CD4+
CD8+
% of responding T cells
15
10
5
0
d: -7 8 48
-7 8 48
b)
CD4+
CD8+
-7
d8
d48
% of responding T cells
40
20
0
60
IL2
IFNγ
TNF
c)
CD56 + - -
CD16 - - +
% of responding NK cells
d: -7 8 48
-7 8 48
-7 8 48
d)
*
*
-7
d8
d48
% of responding NK cells
60
40
20
0
IFNγ
MIP1β
TNF
(Pie slices)
e)
-7
d8
d48
% of responding NK cells
80
60
40
20
0
IFNγ
MIP1β
TNF
(Pie slices)

Figure S2

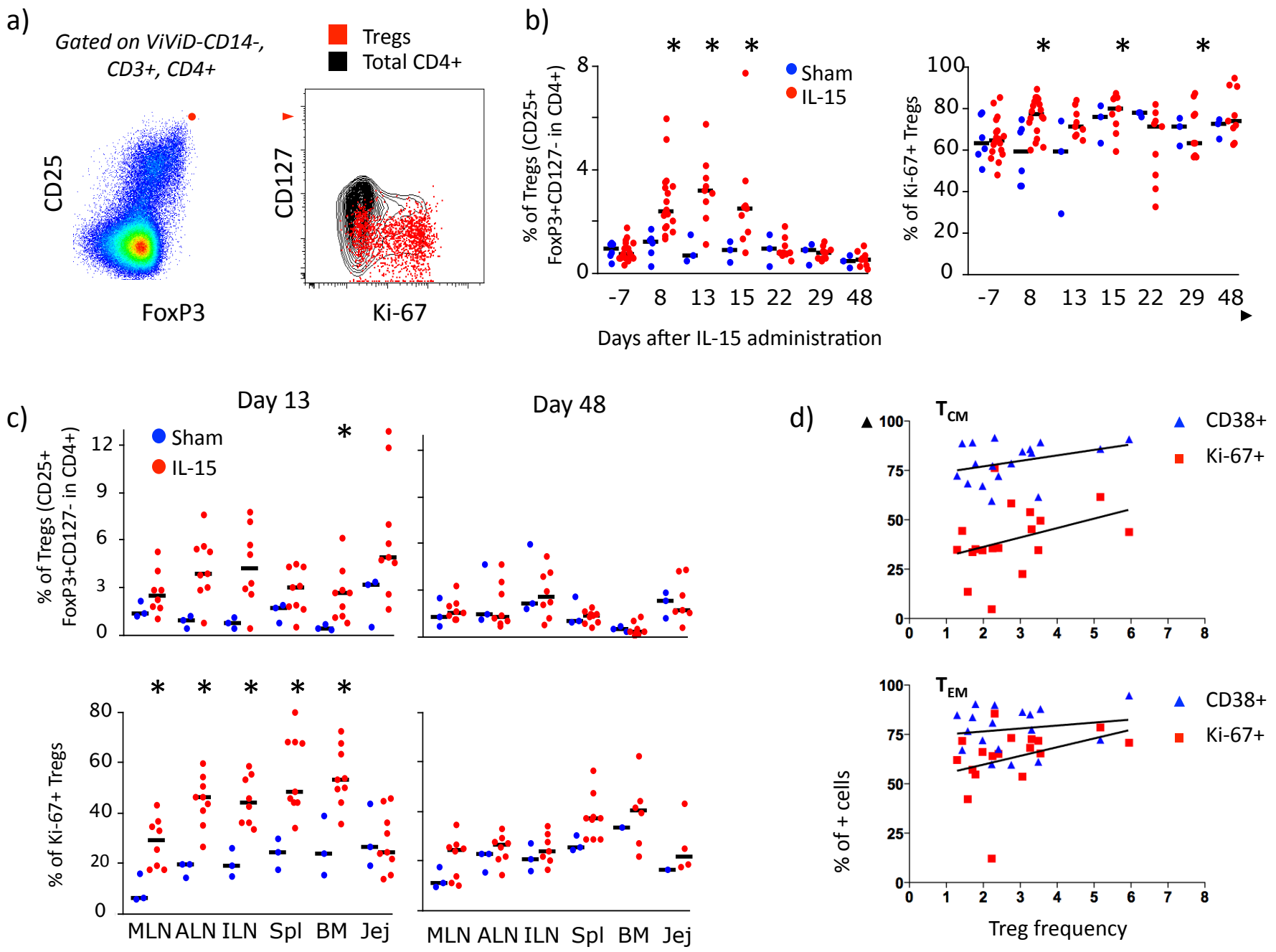
a)
Gated on ViViD-CD14-, CD3+, CD4+
Tregs
Total CD4+
CD25
FoxP3
CD127
Ki-67
b)
Sham
IL-15
% of Tregs (CD25+ FoxP3+CD127- in CD4+)
% of Ki-67+ Tregs
Days after IL-15 administration
c)
Day 13
Day 48
Sham
IL-15
% of Tregs (CD25+ FoxP3+CD127- in CD4+)
% of Ki-67+ Tregs
MLN ALN ILN Spl BM Jej
d)
T_{CM}
T_{EM}
CD38+
Ki-67+
% of + cells
Treg frequency

Figure S3

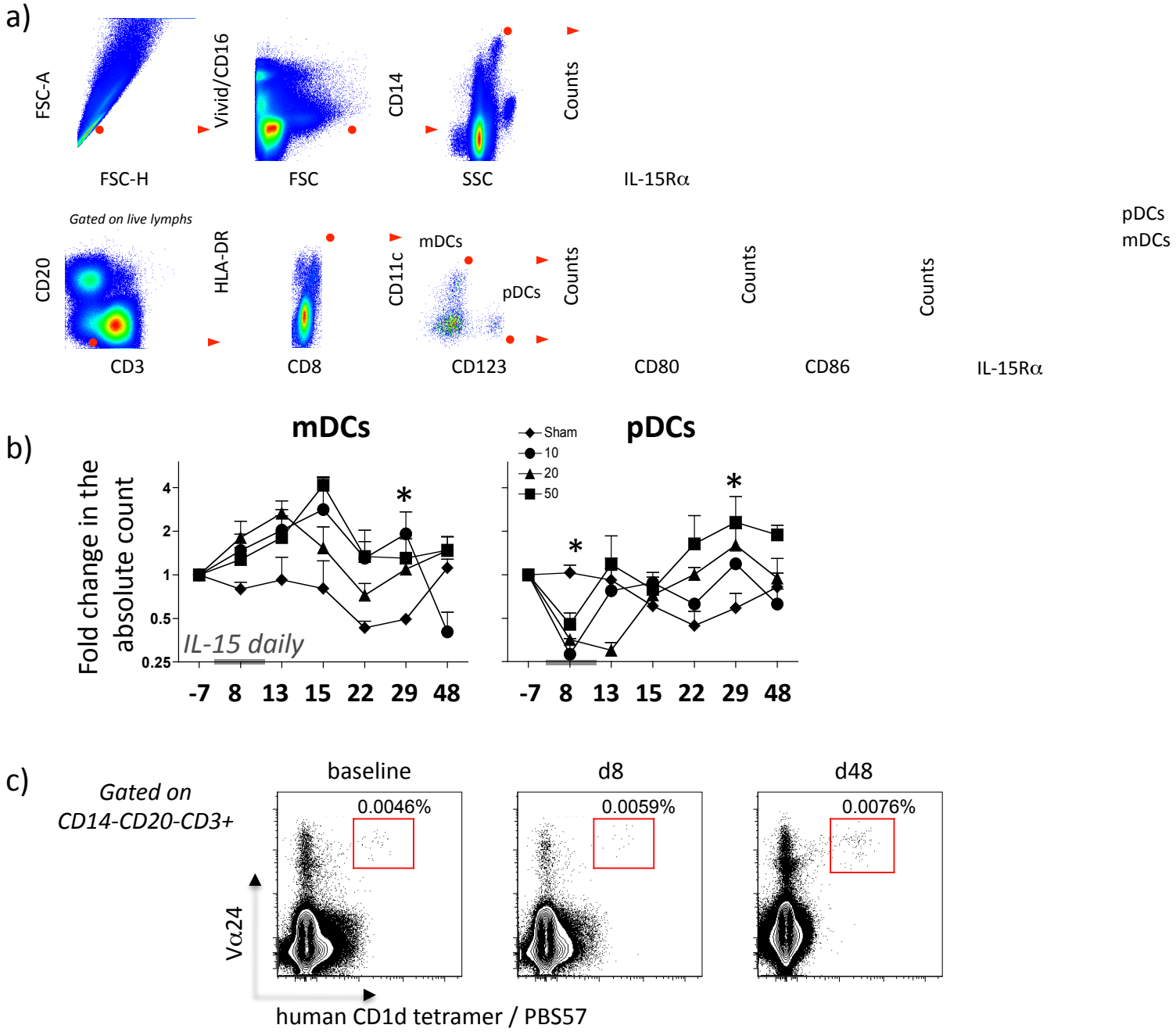
a)
FSC-A
FSC-H
Vivid/CD16
FSC
CD14
SSC
Counts
IL-15Rα
Gated on live lymphs
CD20
CD3
HLA-DR
CD8
CD11c
mDCs
pDCs
CD123
Counts
CD80
Counts
CD86
Counts
IL-15Rα
pDCs
mDCs
b)
mDCs
pDCs
Sham
10
20
50
Fold change in the absolute count
IL-15 daily
-7 8 13 15 22 29 48
c)
Gated on CD14-CD20-CD3+
baseline
d8
d48
0.0046%
0.0059%
0.0076%
Vα24
human CD1d tetramer / PBS57

Figure S4

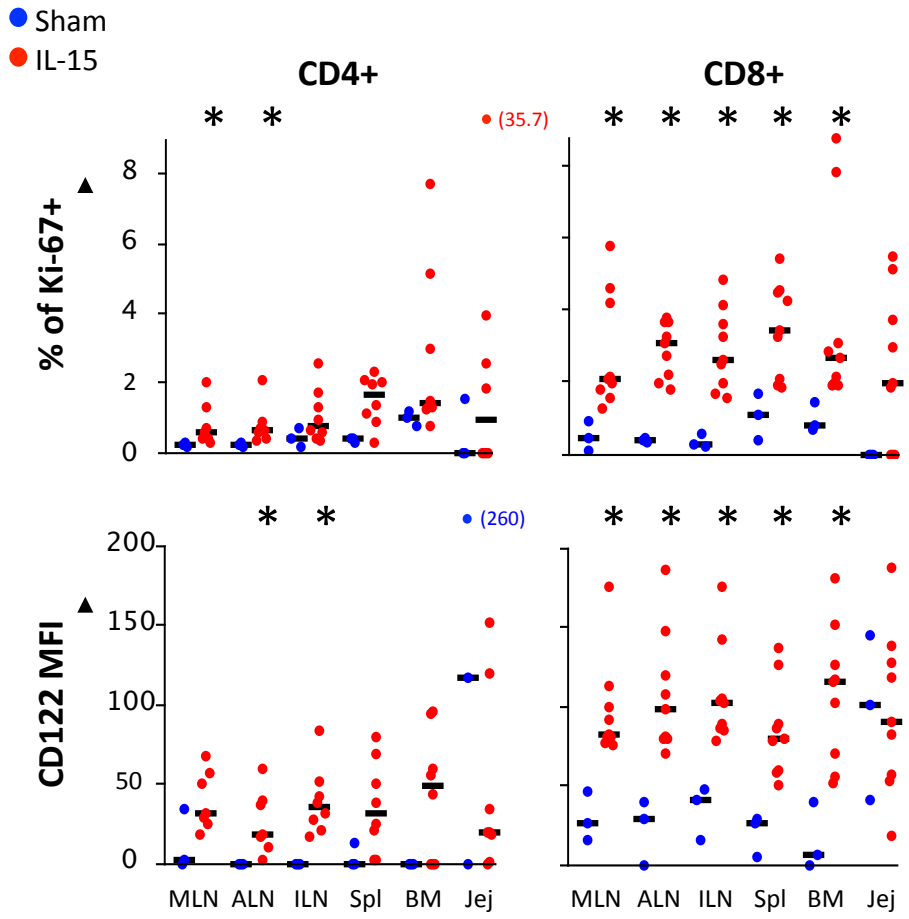
Sham
IL-15
CD4+
CD8+
(35.7)
% of Ki-67+
8
6
4
2
0
(260)
CD122 MFI
200
150
100
50
0
MLN ALN ILN Spl BM Jej
MLN ALN ILN Spl BM Jej

Figure S5

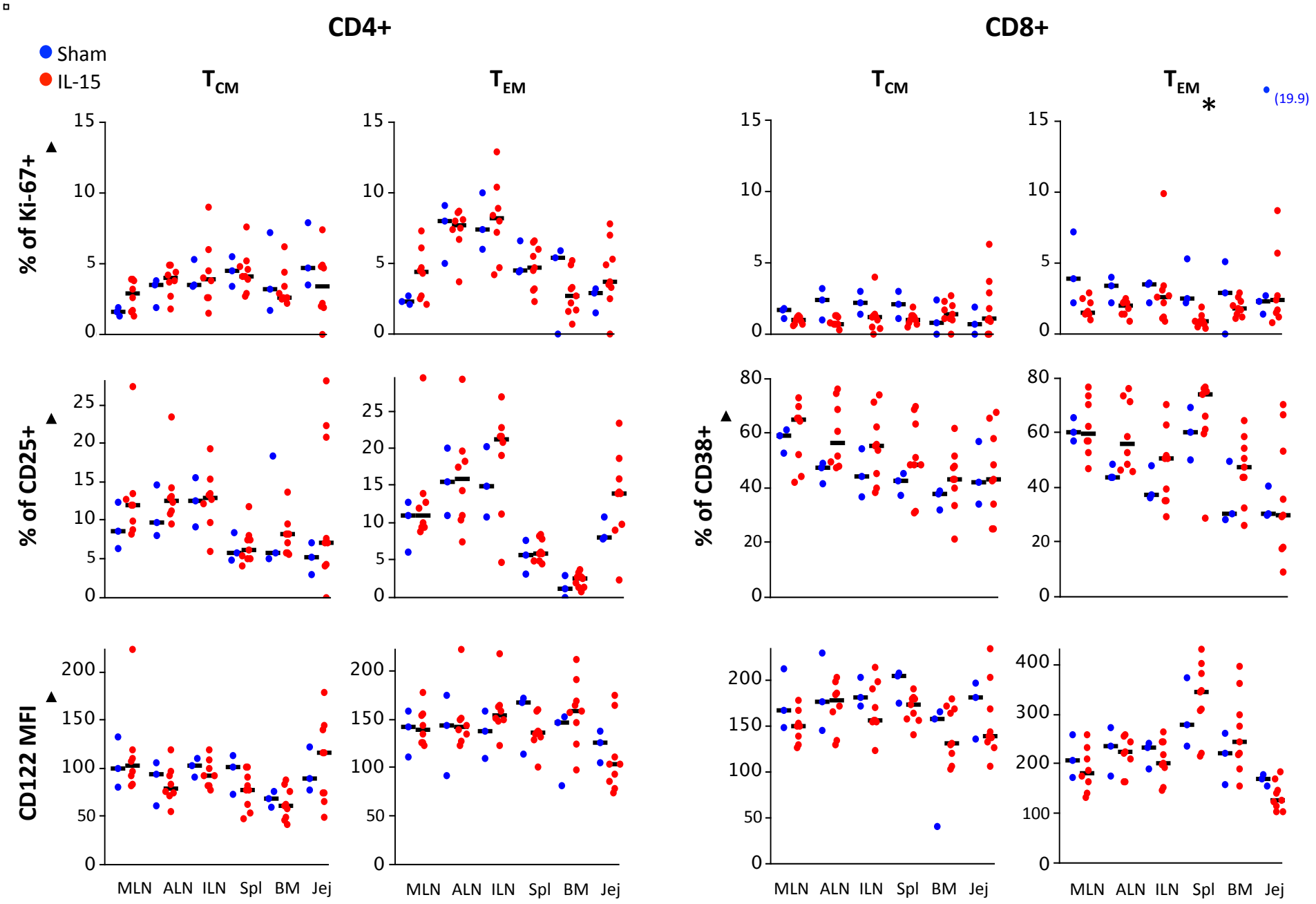
CD4+
CD8+
Sham
IL-15
T CM
T EM
T CM
T EM
*
(19.9)
% of Ki-67+
% of CD25+
% of CD38+
CD122 MFI
MLN ALN ILN Spl BM Jej

Figure S6

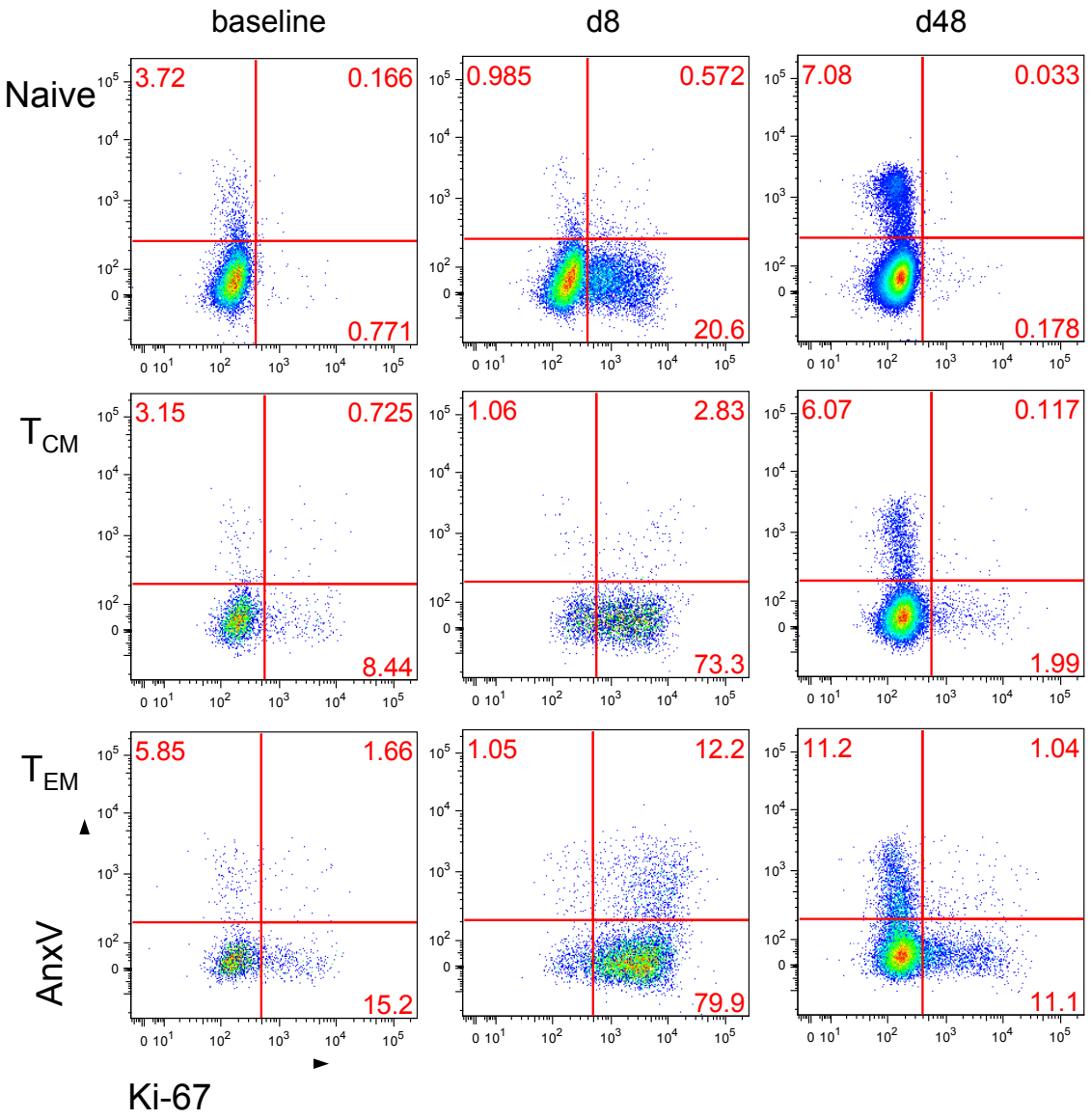
baseline
d8
d48
Naive
T CM
T EM
AnxV
Ki-67
3.72
0.166
0.771
0.985
0.572
20.6
7.08
0.033
0.178
3.15
0.725
8.44
1.06
2.83
73.3
6.07
0.117
1.99
5.85
1.66
15.2
1.05
12.2
79.9
11.2
1.04
11.1

Figure S7